Beyond mean field physics with Bose-Einstein condensates in optical lattices

M. Greiner[1,2], O. Mandel[1,2], A. Altmeyer[1,2],
A. Widera[1,2], T. Rom[1,2], T. W. Hänsch[1,2] and I. Bloch[1,2]
[1] *Sektion Physik, Ludwig-Maximilians-Universität, Munich, Germany*
[2] *Max-Planck-Institut für Quantenoptik, Garching, Germany*

Abstract

By loading Bose-Einstein condensates into a three dimensional optical lattice potential we are able to demonstrate several new intriguing regimes in the physics of ultracold atoms. For example by changing the lattice potential depth we have been able to induce a quantum phase transition from a superfluid to a Mott insulating ground state of the system. Furthermore, by rapidly isolating the different potential wells from each other the collapse and revival of the matter wave field of a Bose-Einstein condensate has been observed.

1 Introduction

Over the last seven years spectacular experiments with atomic Bose-Einstein condensates have demonstrated the remarkable wave-like nature of this new form of matter [1]. A Bose-Einstein condensate can be considered as the perfect realization of a classical matter wave, just as the emitted light from a laser is the perfect realization of a classical electromagnetic wave. However, a quantized field underlies the classical matter wave of a BEC and it is therefore natural to ask whether one can observe effects due to such a quantization.

In this short review we would like to summarize our work on Bose-Einstein condensates in three-dimensional optical lattices. In such a system the quantized structure of the matter wave field indeed leads to dramatic effects in the behavior of ultracold quantum matter. For example, by increasing the lattice potential depth we are able to strongly decrease the kinetic energy in the system, while simultaneously increasing the interaction energy between the atoms in each individual lattice site. Thereby we have been able to convert the system from a weakly interacting Bose gas to a strongly correlated Bose system where interactions between the atoms dominate its behavior. During this process the many body state changes from a superfluid to a Mott insulator, which has been observed in the experiment [2] and was initially predicted in [3]. A similar behavior has also been found in the case of Bose-Einstein condensates in one-dimensional lattices [4] (see also proceeding of M. Kasevich).

In addition we demonstrate experimentally that whenever a BEC is split into two or more parts, such that initially a constant relative phase exists between the matter waves of the two subsystems, these matter waves undergo a series of collapses and revivals, due to the quantized structure of the matter wave field and the coherent interactions between the atoms [5]. Such a behavior was predicted theoretically [6, 7, 8, 9, 10, 11] and is reminiscent to the collapse and revival of Rabi oscillations in the interaction of a single atom with a single-mode radiation field in cavity quantum electrodynamics [12, 13].

2 Section I
Superfluid to Mott insulator transition

2.1 Experimental setup

Starting point for all the experiments are magnetically trapped Bose-Einstein condensates of ^{87}Rb atoms in a new experimental setup with excellent optical access [14]. In order to create a three-dimensional periodic potential we overlap the crossing point of three optical standing waves at the position of the Bose-Einstein condensate. These standing waves are operated at a wavelength of $\lambda = 830 - 850\,\mathrm{nm}$ such that they are red detuned relative to the Rb D1- and D2-atomic resonances. Due to the resulting dipole force [15] the atoms are attracted to the intensity maxima of the light field such that a periodic potential is realized through the optical interference pattern. This periodic potential has a simple cubic lattice structure with a lattice spacing of $\lambda/2$. The potential depth of the optical lattice is naturally measured in units on the recoil energy $E_r = \hbar^2 k^2/2m$, with k being the wave vector of the laser light $k = 2\pi/\lambda$ and m the mass of a single atom. All laser beams are intensity stabilized to provide stable optical potentials during and between different realizations of the experiment. In our setup lattice potential depths of up to $45\,E_r$ can be realized, leading to vibrational frequencies of up to 40 kHz on each lattice site.

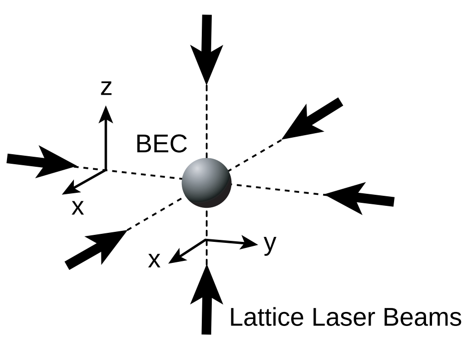

Figure 1: Three orthogonal standing waves are overlapped at the position of the Bose-Einstein condensate to create a three-dimensional periodic potential with simple cubic lattice structure.

2.2 Bose-Hubbard hamiltonian

The behavior of bosonic atoms with repulsive interactions in a periodic potential is fully captured by the Bose-Hubbard hamiltonian of solid state physics, which in the homogeneous case can be expressed through:

$$H = -J \sum_{\langle i,j \rangle} \hat{a}_i^\dagger \hat{a}_j + \frac{1}{2} U \sum_i \hat{n}_i(\hat{n}_i - 1). \tag{1}$$

Here $\hat{a}_i^\dagger$ and $\hat{a}_i$ describe the creation and annihilation operators for a boson on the ith lattice site and $\hat{n}_i$ counts the number of bosons on the ith lattice site. The tunnel coupling between neighboring potential wells is characterized by the tunnel matrix element $J = -\int d^3x w(\mathbf{x} - \mathbf{x}_i)(-\hbar^2\nabla^2/2m + V_{lat}(\mathbf{x}))w(\mathbf{x} - \mathbf{x}_j)$ where $w(\mathbf{x} - \mathbf{x}_i)$ is a single particle Wannier function localized to the ith lattice site and $V_{lat}(\mathbf{x})$ indicates the optical lattice potential. The repulsion between two atoms on a single lattice site is quantified by the on-site matrix element $U = (4\pi\hbar^2 a/m)\int |w(\mathbf{x})|^4 d^3x$, with a being the scattering length of an atom. Due to the short range of the interactions compared to the lattice spacing, the interaction energy is well described by the second term of eq. 1 which characterizes a purely on-site interaction.

2.3 Ground states of the Bose-Hubbard hamiltonian

The Bose-Hubbard hamiltonian of eq. 1 has two distinct ground states depending on the strength of the interactions U relative to the tunnel-coupling J. In order to gain insight into the two limiting ground-states, let us first consider the case of a double well system with only two interacting neutral atoms.

2.3.1 Double well case

In the double well system the two lowest lying states for non-interacting particles are the symmetric $|\varphi_S\rangle = 1/\sqrt{2}(|\varphi_L\rangle + |\varphi_R\rangle)$ and the anti-symmetric $|\varphi_A\rangle = 1/\sqrt{2}(|\varphi_L\rangle - |\varphi_R\rangle)$ states, where $|\varphi_L\rangle$ and $|\varphi_R\rangle$ are the ground states of the left and right hand side of the double well potential. The energy difference between $|\varphi_S\rangle$ and $|\varphi_A\rangle$ will be named J, which characterizes the tunnel coupling between the two wells and depends strongly on the barrier height between the two potentials.

In case of no interactions, the ground state of the two-body system is realized when each atom is in the symmetric ground state of the double well system (see Fig. 2a). Such a situation yields an average occupation of one atom per site with the single site many body state actually being in a superposition of zero, one and two atoms. Let us now consider the effects due to a repulsive interaction between the atoms. If both atoms are again in the symmetric ground state of the double well, the total energy of such a state will increase due to the repulsive interactions between the atoms. This higher energy cost is a direct consequence of having contributions where both atoms occupy the same site of the double well. This leads to an interaction energy of $1/2U$ for this state.

If this energy cost is much greater than the splitting J between the symmetric and anti-symmetric ground states of the noninteracting system, the system can minimize its energy when each atom is in a superposition of the symmetric and antisymmetric ground state of the double well $1/\sqrt{2}(|\varphi_S\rangle \pm |\varphi_A\rangle)$. The resulting many body state can then be written as $|\Psi\rangle = 1/\sqrt{2}(|\varphi_L\rangle \otimes |\varphi_R\rangle + |\varphi_R\rangle \otimes |\varphi_L\rangle)$. Here exactly one atom occupies the left and right site of the double well. Now the interaction energy vanishes because both atoms never occupy the same lattice site. The system will

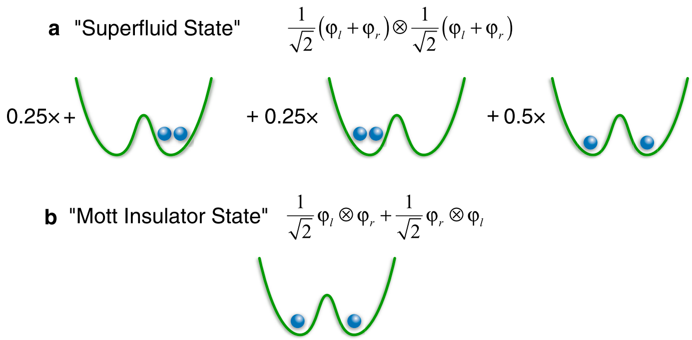

Figure 2: Ground state of two interacting particles in a double well. For interaction energies U smaller than the tunnel coupling J the ground state of the two-body system is realized by the "superfluid" state **a**. If on the other hand U is much larger than J, then the ground state of the two-body system is the Mott insulating state **b**.

choose this new "Mott insulating" ground state when the energy costs of populating the antisymmetric state of the double well system are outweighed by the energy reduction in the interaction energy. It is important to note that precisely the atom number fluctuations due to the delocalized single particle wave functions make the "superfluid" state unfavorable for large U.

Such a change can be induced by adiabatically increasing the barrier height in the double well system, such that J decreases exponentially and the energy cost for populating the antisymmetric state becomes smaller and smaller. Eventually it will then be favorable for the system to change from the "superfluid" ground state, where each atom is delocalized over the two wells, to the "Mott insulating" state, where each atom is localized to a single lattice site.

2.3.2 Multiple well case

The above ideas can be readily extended to the multiple well case of the periodic potential of an optical lattice. For $U/J \ll 1$ the tunnelling term dominates the hamiltonian and the ground-state of the many-body system with N atoms is given by a product of identical single particle Bloch waves, where each atom is spread out over the entire lattice with M lattice sites:

$$|\Psi_{SF}\rangle_{U/J\approx 0} \propto \left(\sum_{i=1}^{M} \hat{a}_i^\dagger\right)^N |0\rangle. \tag{2}$$

Since the many-body state is a product over identical single particle states, a macroscopic wave function can be used to describe the system. Here the single site many-body wave function $|\phi\rangle_i$ is almost equivalent to a coherent state. The atom number per lattice site then remains uncertain and follows a Poissonian distribution with a Variance given by the average number of atoms on this lattice site $\mathrm{Var}(n_i) = \langle \hat{n}_i \rangle$. The non-vanishing expectation value of $\psi_i = \langle \phi_i | \hat{a}_i | \phi_i \rangle$ then characterizes the coherent matter wave field on the ith lattice site. This matter wave field has a fixed phase relative to all other coherent matter wave fields on different lattice sites.

If, on the other hand, interactions dominate the behavior of the hamiltonian, such that $U/J \gg 1$, then fluctuations in the atom number on a single lattice site become energetically costly and the ground state of the system will instead consist of localized atomic wave functions that minimize the interaction energy. The many-body ground state is then a product of local Fock states for each lattice site. In this limit the ground state of the many-body system for a commensurate filling of n atoms per lattice site is given by:

$$|\Psi_{MI}\rangle_{J\approx 0} \propto \prod_{i=1}^{M} (\hat{a}_i^\dagger)^n |0\rangle. \tag{3}$$

Under such a situation the atom number on each lattice site is exactly determined but the phase of the coherent matter wave field on a lattice site has obtained a maximum uncertainty. This is characterized by a vanishing of the matter wave field on the ith lattice site $\psi_i = \langle\phi_i|\hat{a}_i|\phi_i\rangle \approx 0$.

In this regime of strong correlations, the interactions between the atoms dominate the behavior of the system and the many body state is not amenable anymore to a description as a macroscopic matter wave, nor can the system be treated by the theories for a weakly interacting Bose gas of Gross, Pitaevskii and Bogoliubov.

2.4 Superfluid-Mott insulator transition

In the experiment the crucial parameter U/J that characterizes the strength of the interactions relative to the tunnel coupling between neighboring sites can be varied by simply changing the potential depth of the optical lattice potential. By increasing the lattice potential depth, U increases almost linearly due to the tighter localization of the atomic wave packets on each lattice site and J decreases exponentially due the decreasing tunnel coupling. The ratio U/J can therefore be varied over a large range from $U/J \approx 0$ up to values in our case of $U/J \approx 2000$.

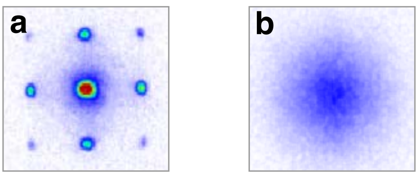

Figure 3: Absorption images of multiple matter wave interference patterns after releasing the atoms from an optical lattice potential with a potential depth of **a** $7\,E_r$ and **b** $20\,E_r$. The ballistic expansion time was 15 ms.

In the superfluid regime [16] phase coherence of the matter wave field across the lattice characterizes the many body state. This can be observed by suddenly turning off all trapping fields, such that the individual matter wave fields on different lattice sites expand and interfere with each other. After a fixed time of flight period the

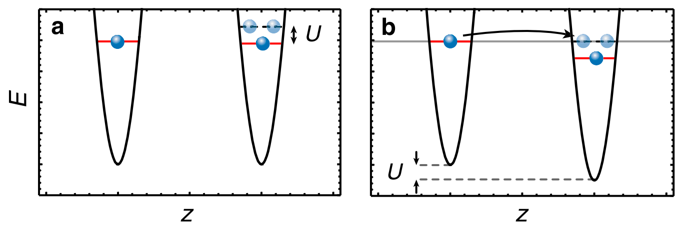

Figure 4: **a** Excitation gap in the Mott insulator phase with exactly $n = 1$ atom on each lattice site. **b** If a correct potential gradient is added, atoms can tunnel again.

atomic density distribution can then be measured by absorption imaging. Such an image directly reveals the momentum distribution of the trapped atoms. In Fig. 3a an interference pattern can be seen after releasing the atoms from a three-dimensional lattice potential.

If on the other hand the optical lattice potential depth is increased such that the system is in the Mott insulating regime, phase coherence is lost between the matter wave fields on neighboring lattice sites due to the formation of Fock states [3, 17, 18]. In this case no interference pattern can be seen in the time of flight images. (see Fig. 3b).

In addition to the fundamentally different momentum distributions in the superfluid and Mott insulating regime, the excitation spectrum is markedly different as well in both cases. Whereas the excitation spectrum in the superfluid regime is gapless, it is gapped in the Mott insulating regime. This energy gap of order U can be attributed to the now localized atomic wave functions of the atoms.

Let us consider for example a Mott insulating state with exactly one atom per lattice site. The lowest lying excitation to such a state is determined by removing an atom from a lattice site and placing it into the neighboring lattice site (see Fig. 4a). Due to the onsite repulsion between the atoms, however, such an excitation costs energy U which is usually not available to the system. Therefore these are only allowed in virtual processes and an atom in general has to remain immobile at its original position. If one adds a potential gradient such that the energy difference between neighboring lattice sites ΔE exactly matches the onsite energy cost U, then such an excitation becomes energetically possible and one is able to resonantly perturb the system (see Fig. 4b). We have been able to measure this change in the excitation spectrum by applying varying magnetic field gradients to the system for different lattice potential depths and detecting the response of the system to such perturbations [2, 19].

3 Section II
Collapse and revival of the matter wave field of a Bose-Einstein condensate

A long standing question in interacting macroscopic quantum systems has been directed towards the problem of what happens to an initially well defined relative phase between two macroscopic quantum systems after they have been isolated from each other. Equivalently one may ask: how do the individual macroscopic quantum fields evolve after they have been isolated from each other? Such a situation can be realized for example with a Bose-Einstein condensate that is split into two parts, such that a constant relative phase is initially established between the two subsystems BEC1 and BEC2 (see Fig. 5).

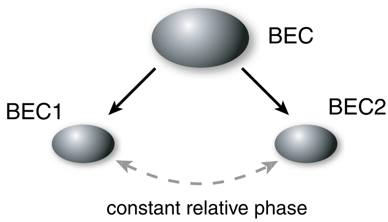

Figure 5: A Bose-Einstein condensate is split into two parts with an initially constant phase between the two subsystems BEC1 and BEC2.

Whenever a condensate is split into two parts such that a fixed relative phase is established between those two parts, the many body state in each of the BECs is in a superposition of different atom number states. Let us now consider the case of repulsive interactions between the atoms and determine how such superpositions of atom number states evolve over time, taking into account the collisions between the atoms. Let us first assume that all atoms in a subsystem occupy the ground state of its external confining potential. If the interaction energy is then small compared to the vibrational spacing in this potential well, the hamiltonian governing the behavior of the atoms is given by:

$$H = \frac{1}{2} U \hat{n}(\hat{n} - 1). \tag{4}$$

The eigenstates of the above hamiltonian are Fock states $|n\rangle$ in the atom number, with eigenenergies $E_n = Un(n-1)/2$. The evolution with time of such an n-particle state is then simply given by $|n\rangle(t) = |n\rangle(0) \times \exp(-iE_n t/\hbar)$.

If the atoms in such a subsystem are brought into a superposition of atom number states $|n\rangle$, which always occurs whenever a fixed relative phase persists between the two subsystems, each subsystem is in a superposition of eigenstates $|n\rangle$ which results in a dynamical evolution of this state over time. Let us consider for example a coherent state $|\alpha\rangle = \exp(-|\alpha|^2/2) \sum_n \frac{\alpha^n}{\sqrt{n!}} |n\rangle$ in each subsystem [20]. Here α is the amplitude of the coherent state with $|\alpha|^2$ corresponding to the average atom number in the subsystem. The evolution with time of such a coherent state can be evaluated by taking into account the time evolution of the different Fock states forming the coherent state:

$$|\alpha\rangle(t) = e^{-|\alpha|^2/2} \sum_n \frac{\alpha^n}{\sqrt{n!}} e^{-i\frac{1}{2}Un(n-1)t/\hbar} |n\rangle. \tag{5}$$

The coherent matter wave field ψ in each of the subsystems can then simply be evaluated through $\psi = \langle \alpha(t)|\hat{a}|\alpha(t)\rangle$, which exhibits an intriguing dynamical evolution [6, 7, 8, 9, 10]. At first, the different phase evolutions of the atom number states

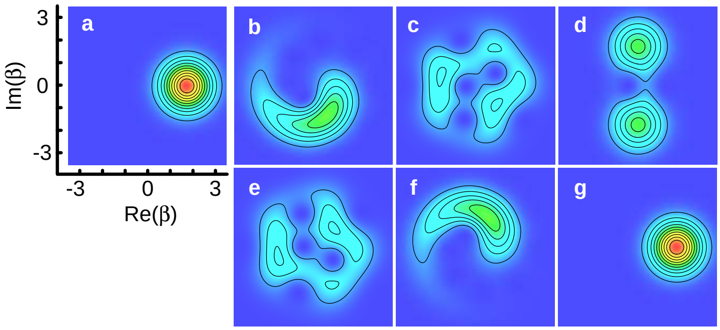

Figure 6: Calculated quantum dynamics of an initially coherent state with an average number of three atoms due to the coherent cold collisions between the atoms. The graphs show the overlap of the dynamically evolved input state with an arbitrary coherent state of amplitude β. Evolution times are **a** $0\,h/U$; **b** $0.1\,h/U$;**c** $0.4\,h/U$;**d** $0.5\,h/U$;**e** $0.6\,h/U$;**f** $0.9\,h/U$; and **g** h/U.

lead to a collapse of ψ. However, at integer multiples in time of h/U all phase factors in the above equation re-phase modulo 2π and thus lead to a revival of the initial coherent state (see also Fig. 6). The collapse and revival of the coherent matter wave field of a BEC is reminiscent to the collapse and revival of the Rabi oscillations in the interaction of a single atom with a single mode electromagnetic field in cavity quantum electrodynamics [12, 13]. There, the nonlinear atom-field interaction induces the collapse and revival of the Rabi oscillations whereas here the nonlinearity due to the interactions between the atoms themselves leads to the series of collapse and revivals of the matter wave field. It should be pointed out that such a behavior has also been theoretically predicted to occur for a coherent light field propagating in a nonlinear medium [21, 22, 23] but to our knowledge has never been observed experimentally.

In order to realize a coherent state in a potential well, we again use the optical lattice potential and ramp it to a potential depth V_A, which is still completely in the superfluid regime. Then, for low lattice depths, the many-body state in each potential well is almost equal to that of a coherent state with a corresponding average atom number. In such a situation the phase of the matter wave field on the ith lattice site is fixed relative to the matter wave fields on the other lattice sites. Then, in order to isolate the wells from each other, we rapidly increase the lattice potential depth to V_B with negligible tunnel coupling on a timescale that is fast compared to the tunnelling time h/J in the system. Thereby the atoms do not have time to redistribute themselves during the ramp-up of the optical potential and we preserve the initial atom number distribution on each lattice site. On the other hand, the time scale is slow compared to the oscillation frequencies on each lattice site such that no vibrational excitations are created in the ramp-up process and all atoms remain in the vibrational ground state of each well. Using this method we are able to freeze out the atom number distribution at a potential depth V_A and the dynamics of each of the matter wave fields on different lattice sites is now governed by the Hamiltonian of eq. 4.

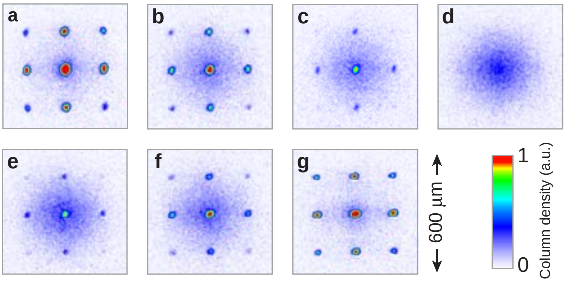

Figure 7: Dynamical evolution of the multiple matter wave interference pattern after jumping from a potential depth $V_A = 8\,E_r$ to a potential depth $V_B = 22\,E_r$ and a subsequent hold time τ. Hold times τ: **a** $0\,\mu$s; **b** $100\,\mu$s; **c** $150\,\mu$s; **d** $250\,\mu$s; **e** $350\,\mu$s; **f** $400\,\mu$s and **g** $550\,\mu$s.

We then follow the dynamical evolution of the matter wave fields by holding the atoms at the lattice potential depth V_B for a variable hold time and then releasing them suddenly from the combined optical and magnetic trapping potentials. After a suitable time of flight period we then take absorption images of the multiple matter wave interference pattern (see Fig. 7). Initially, directly after ramping up the lattice potential, the interference pattern is clearly visible, however after a time of $\approx 250\mu$s the interference pattern is completely lost. Here the vanishing of the interference pattern is caused by the collapse of the matter wave fields on each lattice site. But after a total hold time of 550μs the original interference pattern is regained again, showing that the matter wave fields have revived. It is important to note that the atom number statistics in each of the wells remains constant throughout the dynamical evolution time. This is fundamentally different from the vanishing of the interference pattern in the Mott insulator case, where the atom number distribution changes, but no further dynamical evolution occurs.

The observed collapse and revival of the macroscopic matter wave field of a Bose-Einstein condensate directly demonstrates a striking behavior of ultracold matter beyond mean-field theories that crucially depends on the quantized structure of the matter wave fields and the coherent collisions between the atoms. Furthermore, the collapse times can serve as an independent efficient probe of the atom number statistics in each potential well [5] and the possibility to measure the onsite interaction matrix element U in a frequency measurement should allow high resolution measurements of the scattering length a of different atomic species. Our current experimental efforts are directed to use a state selective movement of atoms in optical lattices together with the coherent collisions, which have been demonstrated here, to realize large scale entanglement in this system [24, 25]. Such a highly entangled state could then serve as a promising new starting ground for quantum computation in optical lattices [26, 27].

References

[1] S. Stringari, C.R. Acad. Sci **4**, 381 (2001).

[2] M. Greiner, O. Mandel, T. Esslinger, T. W. Hänsch, and I. Bloch, Nature **415**, 39 (2002).

[3] D. Jaksch, C. Bruder, J.I. Cirac, C.W. Gardiner, and P. Zoller, Phys. Rev. Lett **81**, 3108 (1998).

[4] C. Orzel, A.K. Tuchman, M.L. Fenselau, M. Yasuda, and M.A. Kasevich, Science **291**, 2386 (2001).

[5] M. Greiner, O. Mandel, T.W. Hänsch, and I. Bloch, Nature **419**, 51 (2002).

[6] E.M. Wright, D.F. Walls, and J.C. Garrison, Phys. Rev. Lett. **77**, 2158 (1996).

[7] E.M. Wright, T. Wong, M.J. Collett, S.M. Tan, and D.F. Walls, Phys. Rev. A **56**, 591 (1996).

[8] A. Imamoglu, M. Lewenstein, and L. You, Phys. Rev. Lett **78**, 2511 (1997).

[9] Y. Castin and J. Dalibard, Phys. Rev. A **55**, 4330 (1997).

[10] J.A. Dunningham, M.J. Collett, and D.F. Walls, Phys. Lett. A **245**, 49 (1998).

[11] W. Zhang and D.F. Walls, Phys. Rev. A **52**, 4696 (1995).

[12] G. Rempe, H. Walther, and N. Klein, Phys. Rev. Lett. **58**, 353 (1987).

[13] M. Brune et al., Phys. Rev. Lett. **76**, 1800 (1996).

[14] M. Greiner, I. Bloch O. Mandel, T.W. Hänsch, and T. Esslinger, Phys. Rev. A **63**, 031401 (2001).

[15] R. Grimm, M. Weidemller, and Yu. B. Ovchinnikov, Adv. At. Mol. Phys. **42**, 95 (2000).

[16] F.S. Cataliotti et al., Science **293**, 843 (2001).

[17] M.P.A. Fisher, P.B. Weichman, G. Grinstein, and D.S. Fisher, Phys. Rev. B **40**, 546 (1989).

[18] S. Sachdev, *Quantum Phase Transitions*, Cambridge Univ. Press, Cambridge, 2001.

[19] S. Sachdev, K. Sengupta, and S.M. Girvin, Phys. Rev. B **66**, 075128 (2002).

[20] D.F. Walls and G.J. Milburn, *Quantum Optics*, Springer, Berlin, 1994.

[21] G.J. Milburn and C.A. Holmes, Phys. Rev. Lett. **56**, 2237 (1986).

[22] B. Yurke and D. Stoler, Phys. Rev. Lett. **57**, 13 (1986).

[23] D.J. Daniel and G.J. Milburn, Phys. Rev. A **39**, 4628 (1989).

[24] D. Jaksch, H.J. Briegel, J.I. Cirac, C.W. Gardiner, and P. Zoller, Phys. Rev. Lett. **82**, 1975 (1999).

[25] H.J. Briegel and R. Raussendorf, Phys. Rev. Lett. **86**, 5188 (2001).

[26] H.J. Briegel, T. Calarco, D. Jaksch, J.I. Cirac, and P. Zoller, J. Mod. Opt. **47**, 415 (2000).

[27] R. Raussendorf and H.J. Briegel, Phys. Rev. Lett. **86**, 5188 (2001).